INTERNATIONAL WORKSHOP on TROPICAL CYCLONES

November 9, 2018

Sub-Topic 4.1
Analysis and prediction of wind field asymmetry

Rapporteur: Charles Sampson

                Naval Research Laboratory

Email: Buck.Sampson@nrlmry.navy.mil

Phone: +1-831-656-4714

Working group: Derrick Herndon (CIMSS), Brian Strahl (JTWC), Liz Ritchie-Tyo (UNSW), Shuji Nishimura and Yohko Igarashi (RSMC Tokyo), John Knaff (NESDIS), Chris Landsea (NHC), Joe Courtney (BoM)

Abstract: Great strides have been made in real-time analysis and forecasting of the surface wind field asymmetries in the last four years, mostly leading to improvements in forecasts of gale wind radii. New observation platforms, new algorithms, advances in NWP, and the capability to bring information to operations have all contributed to these improvements. This chapter summarizes many of the recent changes and improvements to guidance available at a few operational centers.

4.1.1   **Introduction**

In operations, analyzing and forecasting tropical cyclone (TC) wind structure has been one of the biggest challenges at the forecast centers, particularly in those areas without the benefit of aircraft reconnaissance. Wind structure analyses and forecasts are generally provided by forecast centers as "wind radii". These wind radii vary, but are generally defined as the maximum extent of some threshold wind speed in terms of circles, semi-circles, or compass quadrants (northeast, southeast, southwest and northwest) surrounding the TC. The critical thresholds used are generally for gales (17 m/s or 34 kt), storm force (25 m/s or 48 kt), and hurricane force (33 m/s or 64 kt) radii. At some centers an intense TC can require up to 12 estimates (four quadrants for each of the three radii thresholds) for an analysis (0 h) and then 12 estimates for each of the 7 forecast periods (12, 24, 36, 48, 72, 96, and 120 h) for a total of 96 wind radii. Production of such a large number of estimates in real-time can become a time

consuming task. Nonetheless, wind radii estimates are important for post-processed guidance such as wind speed probabilities (e.g., DeMaria et al. 2013; Courtney and Burton 2018), storm surge and wave forecasts (e.g., Sampson et al. 2010; Courtney and Burton 2018), modeling of potential infrastructure damages (e.g., Quiring et al. 2014), wind and wave/surge damage potential (e.g., Powell and Reinhold 2007), and danger swaths and Tropical Cyclone Conditions of Readiness (e.g., Sampson et al. 2012). They are also used to initialize numerical weather models, resulting in some forecast error reduction (Davidson et al. 2014, Tallapragada et al. 2015, Kunii 2015, Bender et al. 2017).

4.1.2 Gale Wind Radii Estimates

The best observed TC wind fields are in the North Atlantic basin where aircraft reconnaissance is available about 30% of the time (Rappaport et al. 2009), more often when landfall is a threat. These observations include flight-adjusted winds, dropsondes, and the Stepped Frequency Microwave Radiometer (SFMR). Scatterometry is used extensively for verification as it is one of the best methods to construct wind radii analyses around TCs, especially when aircraft-based data isn't available. The footprints of the scatterometers cover large areas of the ocean, provide useful estimates of wind speeds less than 25 m/s and can be used for gale wind analysis (e.g., Bentamy et al. 2008; Brennan et al. 2009; Chou et al. 2013). However, scatterometer data is less useful for monitoring TC wind field evolution because of its coarse temporal resolution and frequent partial swaths. It is also not useful for wind speeds greater than 25 m/s or in rain areas as the signal attenuates in heavy rain.

Gale wind radii estimation is among the more tractable structure problems. In addition to scatterometer passes, there are infrared (IR) proxies (Knaff et al. 2016), microwave sounder algorithms, multi-satellite platform analyses (Knaff et al. 2011) and NWP models that show skill in analyzing the outer structure of TCs. A consensus value can be calculated using all available estimates, which is useful both for ground truth and real-time forecasts (OBTK in Figure 1 and Sampson et al. 2018). Additional sources of winds have recently become available to operational commands (e.g., those from algorithms using L-band radiometers discussed in detail in Sub-topic 5.1).   These are particularly valuable in the absence of scatterometer or aircraft data. Efforts are also underway to improve NWP analyses of TC winds, which should further improve and stabilize estimates of gale wind radii.

Errors in the best track wind radii have been estimated to be as high as 40% (Landsea and Franklin 2013, Knaff and Sampson 2015), depending on the quality and quantity of the available observational data. Even in instances when scatterometer passes and/or aircraft are present, the estimates can have significant errors. For example, the average difference between the consensus (OBTK) and the JTWC subjective estimates of gale wind radii in Figure 1 is 21 n mi, with a standard deviation of 18 n mi. As suggested by Torn and Snyder (2012), the standard deviation can be used as a measure of the uncertainty, and 18 n mi is about 14% of climatological mean (125 n mi) of the gale wind radii for this data set.
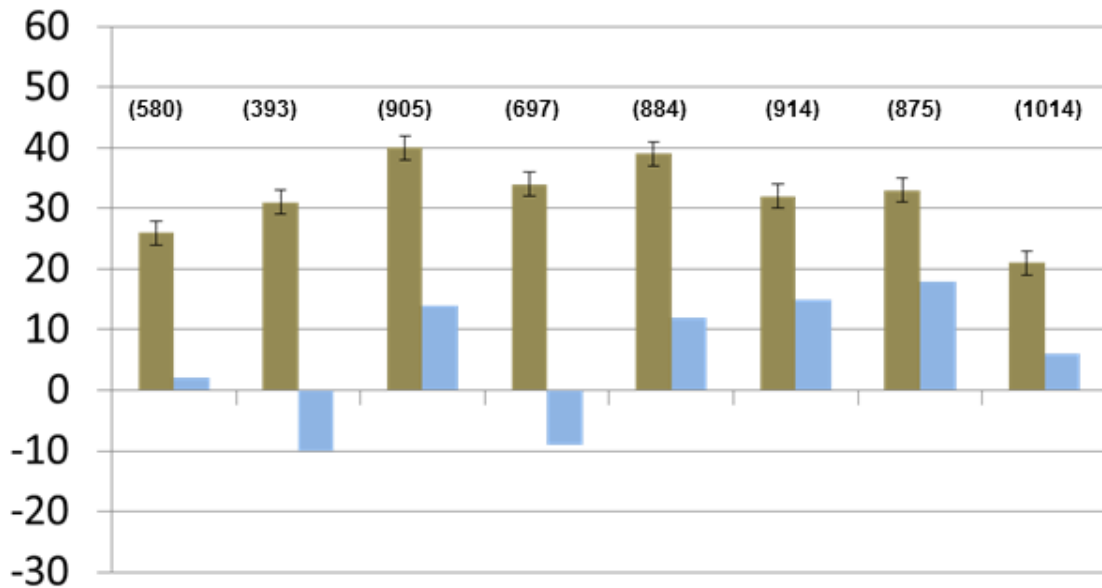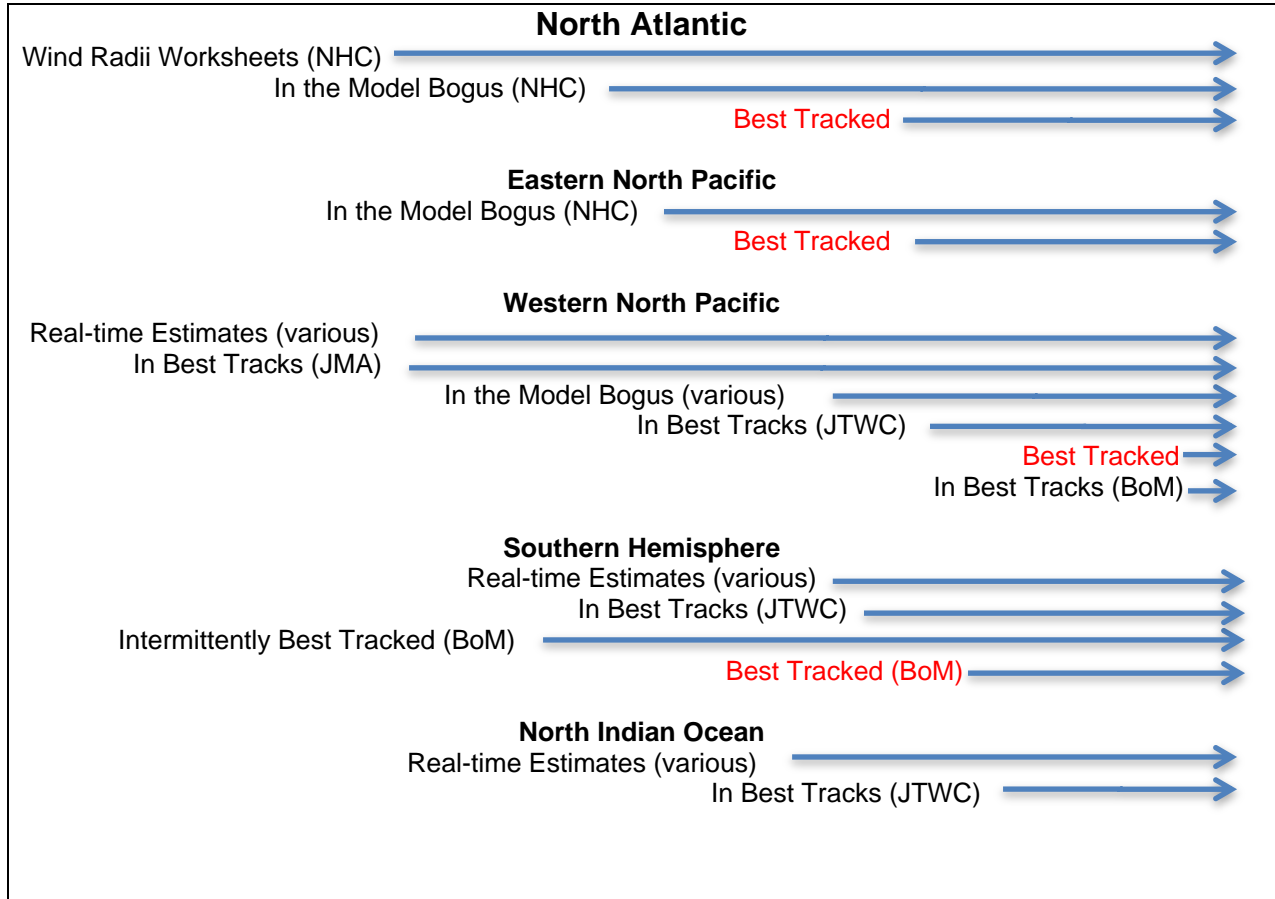
Figure 1.   34-kt wind radii fix mean errors (brown) and biases (blue) relative to JTWC 2014-2016 best tracks coincident with scatterometer fixes (ASCT). OBTK is a mean of the individual estimates. Errors and biases are in n mi and standard error is shown as black bars on means.

Reasonably accurate and continuous estimates of gale wind radii make the wind radii analysis more tenable. Table 1 shows timelines of wind radii estimates at selected operational centers (the timelines start at the initial text and are only approximations). Most of these are real-time estimates, although the National Hurricane Center, Australian Bureau of Meteorology, and Central Pacific Hurricane Center have been consistently including wind radii in their post-season analyses (the so-called "best tracks") since 2004. Others have recently started that effort as well. These best tracks can in turn be used to develop and verify wind radii forecasts as well as downstream applications that rely on wind radii. A note of caution: Each agency will have its own procedures to vet wind radii and those procedures could change in time as new sensors and estimates become available and others are deprecated. Researchers developing algorithms, evaluating performance or constructing trend analysis should contact the individual operational centers regarding potential uses and issues with their data. For example, the JTWC best tracks have subjective post-analysis for the gale wind radii only at present. The NHC post-season analysis currently applies to gale, storm force, and hurricane force wind radii, but not eye diameter or radius of maximum winds. The Australian Bureau of Meteorology wind radii were analyzed post-season through some of the past three decades, but only consistently over the last 15 years.

Table 1

Wind Radii Record Timelines for Selected Operational Centers

1980	1985	1990	1995	2000	2005	2010	2015

North Atlantic
Wind Radii Worksheets (NHC) ────────────────────────────➤
In the Model Bogus (NHC) ──────────────────────➤
Best Tracked ──────────➤

Eastern North Pacific
In the Model Bogus (NHC) ──────────────────────➤
Best Tracked ──────────➤

Western North Pacific
Real-time Estimates (various) ────────────────────────────➤
In Best Tracks (JMA) ────────────────────────────➤
In the Model Bogus (various) ────────────➤
In Best Tracks (JTWC) ────────➤
Best Tracked ➤
In Best Tracks (BoM) ➤

Southern Hemisphere
Real-time Estimates (various) ──────────────➤
In Best Tracks (JTWC) ──────────➤
Intermittently Best Tracked (BoM) ────────────────➤
Best Tracked (BoM) ──────────➤

North Indian Ocean
Real-time Estimates (various) ──────────➤
In Best Tracks (JTWC) ──────➤

4.1.3 **Gale Wind Radii Forecasts**

The Wind Radii CLIPER (DRCL; Knaff et al. 2007) is based on a parametric vortex and has been used both as a skill baseline and a first guess for wind radii forecasts. The DRCL inner core wind radii (i.e., 25 m/s and 33 m/s) are prescribed and so do not suffer from the model resolution issues seen in NWP models. The western North Pacific DRCL has recently been redeveloped with the quality controlled best track data from JTWC (Knaff et al. 2018) and is now more competitive with the NWP model radii in terms of biases. The new DRCL also retains more of the initial wind asymmetry through the forecast.

A statistical-dynamical model has also been developed for most basins (Knaff et al. 2017) that is competitive with NWP model guidance (DSHA in Fig. 2). This model uses

the SHIPS (DeMaria et al. 2005) large scale diagnostics files along with IR imagery and current TC information to predict the TC size change. It is currently run operationally at the Joint Typhoon Warning Center for the western North Pacific, the Southern Hemisphere and the northern Indian Ocean. As with DRCL, this guidance is not directly affected by NWP model resolution.

Figure 2 shows an evaluation of gale wind radii of six operationally available forecast aids and an equally weighted average or "consensus" of the forecasts (RVCN). The consensus has the lowest mean forecast errors and smallest mean biases for the sample. This is in line with findings for other parameters such as track and intensity.
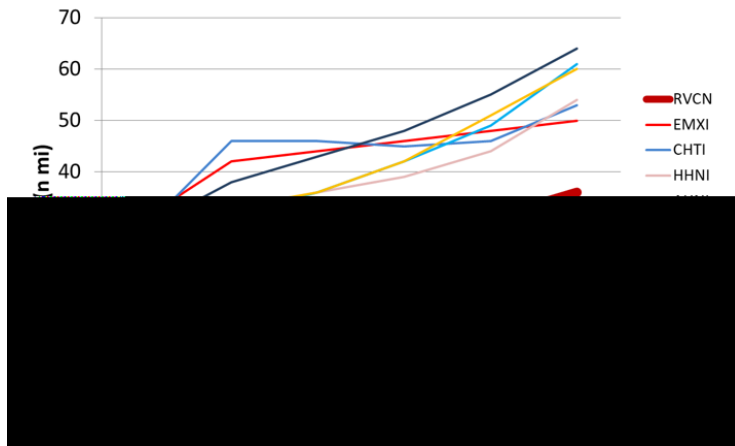
Figure 2. Consensus (RVCN) gale wind radii forecast performance using reanalyzed JTWC best tracks as ground truth for 2014-2016 western North Pacific seasons. Acronyms are as defined at the end of this sub-topic.

The errors associated with the forecasts can be estimated similar to track consensus forecasts. In Fig. 3 a case is shown where RVCN model forecasted the gale wind radius to double in size in the northwest quadrant and then shrink as the TC decayed. The dashed lines (Sampson et al. 2018) indicate the 67th percentile of the predicted error, which in this case contained the post-season best track through the 48-h forecast. The consensus and spread can be used in tandem. The consensus is difficult to beat and can serve as a baseline, with the spread indicating reasonable deviations from the
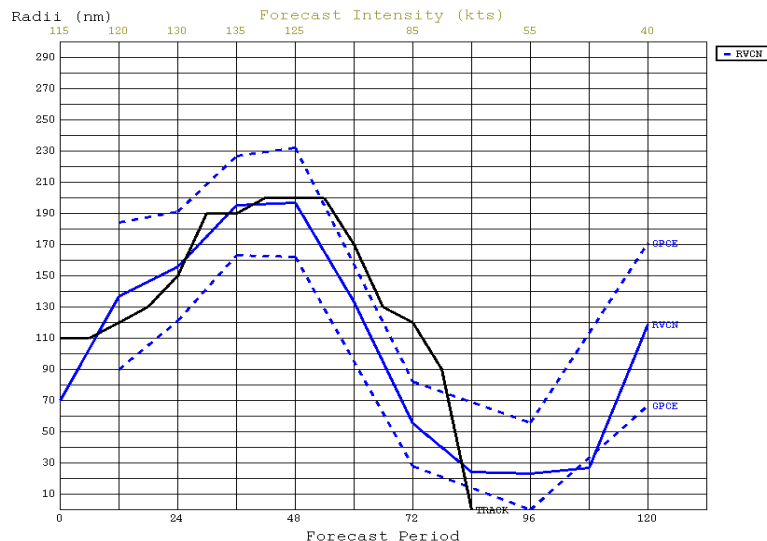

Figure 3. Gale wind radii forecast for the northwest quadrant of MERANTI (2016) on September 12th at 0000 UTC. The blue line is the consensus forecast, dashed lines indicate the 67th percentile of predicted error, and the black line is the post-season best tracked radius. The Joint Typhoon Warning Center forecast intensity (kts) is shown at the top of the chart.

baseline.

4.1.4 Inner Core Estimates and Forecasts

Accurate location of the TC center position is critical in estimating TC structure parameters. The center location uncertainty can exceed 100 km at times and operational centers generally only report center locations every six hours. Errors of this magnitude are on the scale of the inner core radii so this can be a major issue for automated inner core radii estimates. The Automated Rotational Center Hurricane Retrieval (ARCHER) algorithm developed by Wimmers and Velden (2010, 2015) is one possible way to address TC locations. ARCHER uses a spiral and ring scoring algorithm to objectively locate the TC center using geostationary (IR, visible and near-IR), passive microwave imager, and scatterometer data. ARCHER includes information concerning the fix confidence based on the imagery source, scanning geometry and magnitude of the spiral and ring scores.

Ring scores from ARCHER can be used to estimate the TC eye diameter and probability of an eye from geostationary IR and passive microwave imagery. Eye diameter represents the diameter at sensor height which is 10 km for 89 GHz imagery and 16 km for IR. Using an eyewall slope of 45 degree allows the estimation of surface radius of maximum winds, one of the analyzed parameters from the operational centers.

An important structure change that can modify the TC wind field is secondary eyewall formation (SEF) and the eyewall replacement cycle (ERC). As discussed more thoroughly in chapter 4.2, ERC development often leads to expansion of the TC wind field (Maclay et al. 2008, Sitkowski et al. 2011) affecting all critical wind radii. A step change of the radius of maximum winds also occurs as the outer ring in the TC becomes the primary eyewall and the radius shifts from the inner ring to the outer. The Microwave Probability of ERC (M-PERC) model, which is under development through the Joint Hurricane Testbed program produces probabilities of ERC onset using features derived from ~89 GHz imagery in a logistic regression model. The principle components are derived from brightness temperature ring scores evaluated at each pixel radius of 89 GHz imagery along with the time evolving changes in these candidate rings and the TC wind intensity determined from the real-time Vmax estimates provided by the warning agency. A standalone TC wind intensity model is also provided to show the contribution made by the microwave imagery. The resulting forecast is a probability
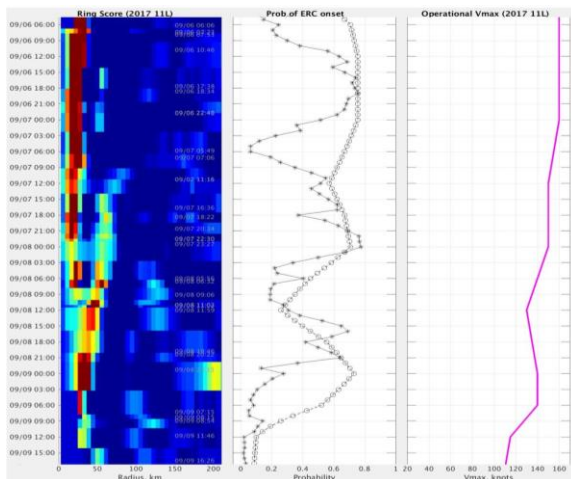

Figure 4. M-PERC table for Hurricane Irma in 2017 displaying Hovmoller diagram of azimuthal rings scores (left), ERC probabilities for the full model (middle solid) and Vmax only (middle dashed), and best track Vmax (right).

of an ERC within 36 h. Figure 4 shows an example of an M-PERC plot for Hurricane Irma in 2017.

A technique that has not yet made it into operations is the DAV (deviation angle variance) technique (Piñeros et al. 2008) for pre-genesis tracking (Rodriguez-Herrera et al. 2015), genesis determination (Wood et al. 2015), intensity estimation (Ritchie et al. 2014), and wind radii estimation (Dolling et al. 2016) for the symmetric or quadrant R34, R50, and R64 radii. The DAV is a parameter that objectively measures the departure of cloud systems in IR imagery from axisymmetry. In particular, the wind radii technique uses the "map of variances" calculated for the entire tropical cyclone to estimate the wind radii in each cardinal quadrant. The model for wind radii is a multiple linear regression model that uses the radius of the highest correlated DAV value along with SST, TC intensity, and the age of the TC since reaching 17 m/s maximum sustained surface winds. The model was developed using the North Atlantic best track dataset and is being developed and tested for the Australian region. Figure 5 shows cross-validation by quadrant and radii for the North Atlantic basin along with simple reconstructed wind fields for Hurricane Ike (2008) with the best track wind radii overlaid in thick contours.
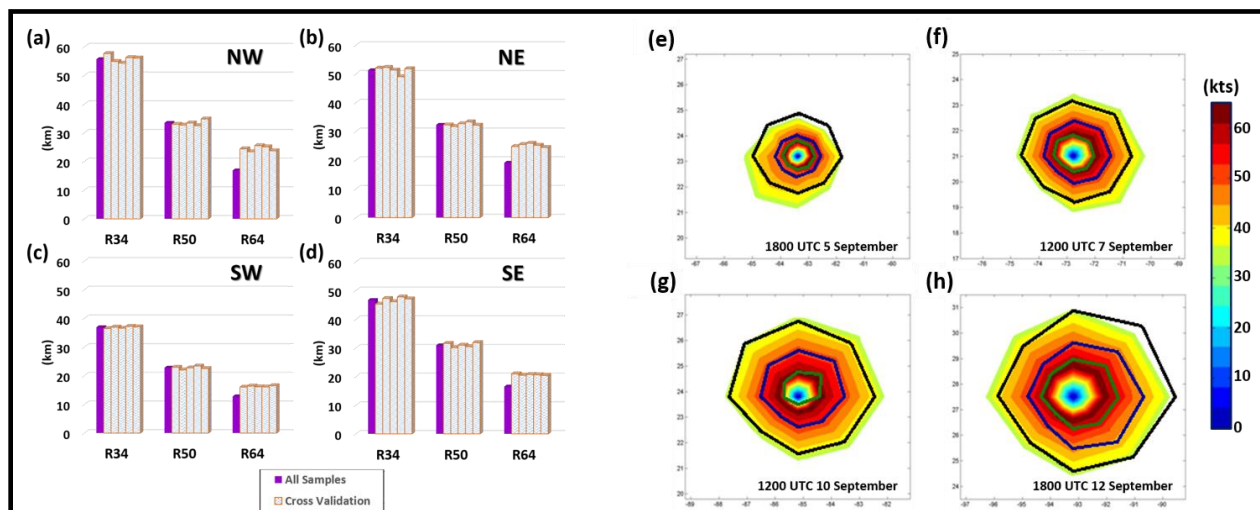

Figure 5. North Atlantic MAE (km) for: (a) northwest; (b) northeast; (c) southwest; and (d) southeast quadrants of the R34, R50, and R64 wind radii for all TCs and for the 5 bins tested during the cross-validation analysis; and (e)-(h) Comparison of the NHC Best Track winds (thick contours, R34-black, R50-blue, R64-green) with the asymmetric regression model (shading) for Hurricane Ike (2008) over .a 7-day period for the 34-, 50-, and 64-kt wind radii [Adapted from Dolling et al. 2016].

4.1.5 Operational Centers Analysis and Forecasting

Japan Meteorological Agency (JMA)

Although scatterometer-derived winds are extremely valuable for TC wind analysis, the relatively small spatial scatterometer footprint, limited temporal coverage (a maximum of

twice daily), sensor saturation in heavy precipitation, and potential biases resulting from the first guess present some limitations. To augment TC surface wind analyses, JMA's Meteorological Satellite Center (MSC) converts low-level Atmospheric Motion Vector (AMV) data from Himawari-8 to surface winds (Nonaka et al. 2016 and Figure 6). Low-level wind speeds are converted to surface winds using 76% of the low-level wind speed and wind directions are adjusted toward the TC center by 9°.

Sea surface AMVs are overlapped with ASCAT winds in daily operations and best-track analysis (Fig. 7). Although these near-surface AMVs are not available under dense clouds, Himawari's 10-minute full-disk refresh rate and high spatial resolution make it possible to estimate strong winds (>15 m/s) in areas surrounding TCs. Forecasters take into consideration the uncertainty in accuracy under deep convection near TC centers, as well as data availability which may differ during day and night depending on the band to use for AMVs. For example, band 03 for visible imagery (B03, 0.64µm) is available only during daytime.
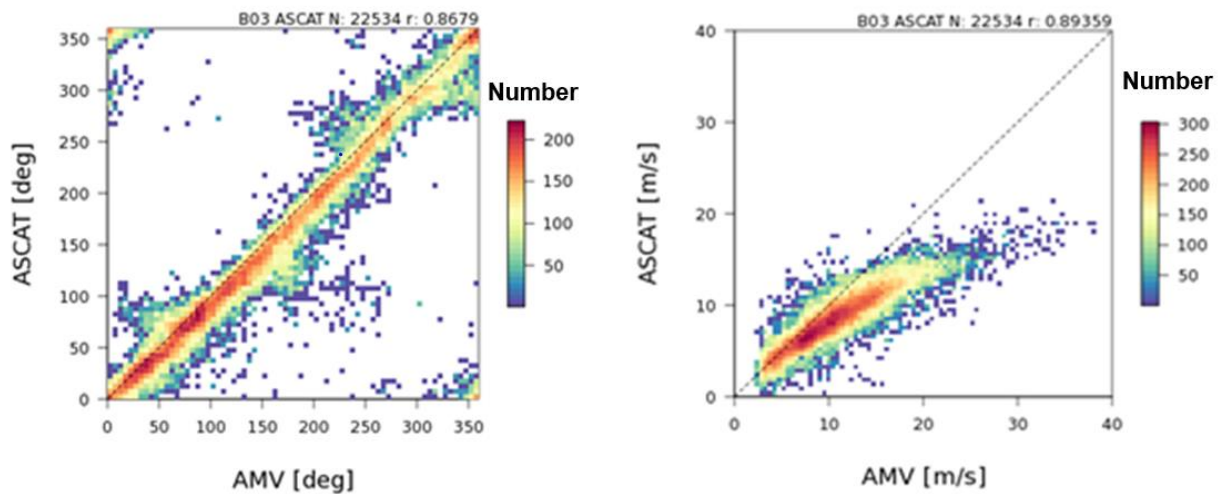

Figure 6. Wind direction (left) and wind speed (right) correlation between low-level AMVs from Himawari-8 B03 and sea surface winds from ASCAT.
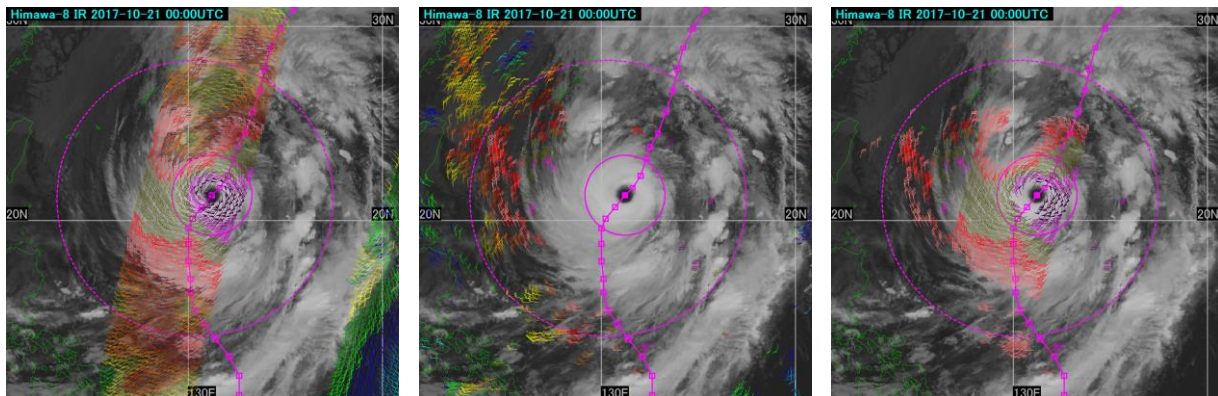

Figure 7. Sea surface AMVs and ASCAT wind composite for Typhoon Lan October 21, 2017 (left: sea surface winds from ASCAT, middle: sea-surface AMVs, right: overlapped for both winds ≥30 kts).

JTWC:

The current JTWC forecast accuracy goals for wind radii specifies that gales and 25 m/s wind radii should be predicted within 20% of the verified values. The addition of new and/or improved analysis and forecast guidance such as OBTK and RVCN described above, as well as improved software, enabled JTWC to extend operational wind radii forecasts from 72 hours to 120 hours in November, 2016. Sampson et al. (2018) found average R34 error for all forecast times to be 15-30%, which is within 10% of the stated JTWC goal for accuracy. Additionally, 120-hour mean forecast R34 errors are now on par with those at 72 hours prior to 2016. Besides the obvious benefit of providing decision makers with additional lead time for gale (R34) and 25 m/s (R50) wind radii that drive U.S. Department of Defense resource protection measures, the consensus of skillful guidance has significantly improved JTWC handling of TC growth throughout a system's lifecycle, particularly during extra-tropical transition. The explicit forecast of 96-h and 120-h wind radii also improves how an algorithm that predicts uncertainty of gale wind radii (the JTWC error swath) conveys these long range uncertainties to DoD users. Prior to 2016 the error swath algorithm was forced to use 72-h wind radii at 96 and 120 h while the current algorithm employs the new JTWC long-range wind radii forecasts. This can be particularly important if the wind radii expand or contract dramatically.

Despite these improvements, operational challenges associated with TC wind structure remain. Because of differences in the timing at which the various analyses or forecasts reach the specified wind thresholds, there may be limited guidance available. This is particularly problematic during the very weak incipient stages of TC development. Another key difficulty is assessing the maximum radius at which winds are no longer attributable to the TC but instead to the large-scale gradient flow. This is a routine consideration for large TCs, such as those that develop out of monsoon depressions or those approaching areas known to have geographically-enhanced channeling of flow such as the Taiwan and Luzon Straits.

NHC:

In the North Atlantic, over the open ocean, the wind radii best tracks are believed to have an uncertainty of around 40, 30, and 25 n mi for 34-, 50-, and 64-kt winds (Landsea and Franklin 2013). Given that these large uncertainties are on the order of about one third to one half of the values they are depicting (Figure 8), routine verification of NHC size forecasts with limited verification data is not currently justified.
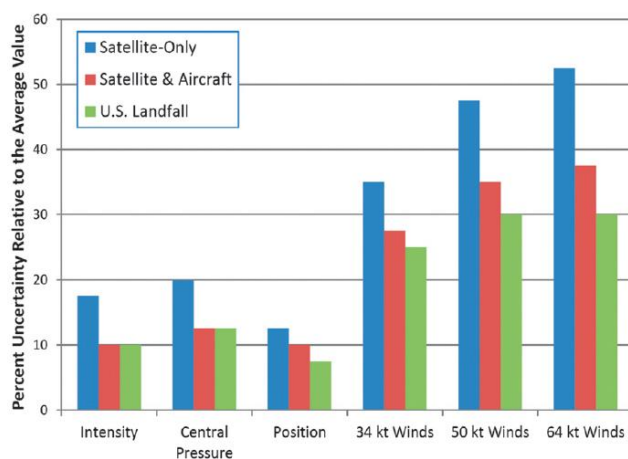

Figure 8: Relative uncertainty in the best tracks for intensity, central pressure, position, 34-, 50-, and 64-kt wind radii for tropical storms and hurricanes. (From Landsea and Franklin 2013).

Cangialosi and Landsea (2016) produced a formal verification of a subset of the NHC wind radii forecasts and selected guidance. The verification of the reconnaissance-only dataset, which was used to get the most accurate "ground truth" information, showed that the NHC wind radii average errors increased with forecast time and were skillful when compared against climatology and persistence. The dynamical models, however, were generally not skillful and had errors that were much larger than the NHC forecasts and mainly had negative biases. It is worth noting, however, that the magnitude of these NHC wind radii errors - especially for the short-term (12, 24, and 36 hour forecasts) for this reconnaissance-only verification was about the same size as the uncertainty in the best track values themselves (Landsea and Franklin 2013). Thus continued development of observational techniques is desired, as these will better assist efforts for both operational and best track assessments of the tropical-storm-force and hurricane-force wind radii. In addition, NHC forecasts of wind radii can be improved by better guidance being made available to the forecasters. This would include improved explicit representation of the tropical cyclone wind field in both global and mesoscale hurricane models, statistical-dynamical approaches, as well consensus techniques (Sampson and Knaff 2015). This last approach – the wind radii variable consensus method (RVCN) – has been available to NHC forecasters during 2017 and 2018 and is quickly becoming the most relied-upon guidance for wind radii predictions.

4.1.6 Conclusions

From an operational perspective, great strides are being made in both analysis and forecasting of surface wind structure. The last four years have seen new and improved algorithms for estimating surface winds in the vicinity of TCs. Improvements in NWP data assimilation and forecasting have yielded guidance for analysis, forecast and forecast error estimates of gale wind radii and possibly inner core radii. The expectation is that we should see further improvement in wind radii and wind radii asymmetry estimates as algorithms from new observing platforms (e.g., L-band radiometers discussed in Sub-topic 5.1 and shown below in Figure 9) gain acceptance in the operational community, and we should see further improvements in wind radii forecasting as NWP models improve and new guidance on inner core radii (e.g., M-PERC and DAV) are used more effectively. Validation of inner core radii estimates and forecasts remains difficult due to the paucity of observations, but there is hope that new sensors and algorithms to address inner core radii will help alleviate this problem.
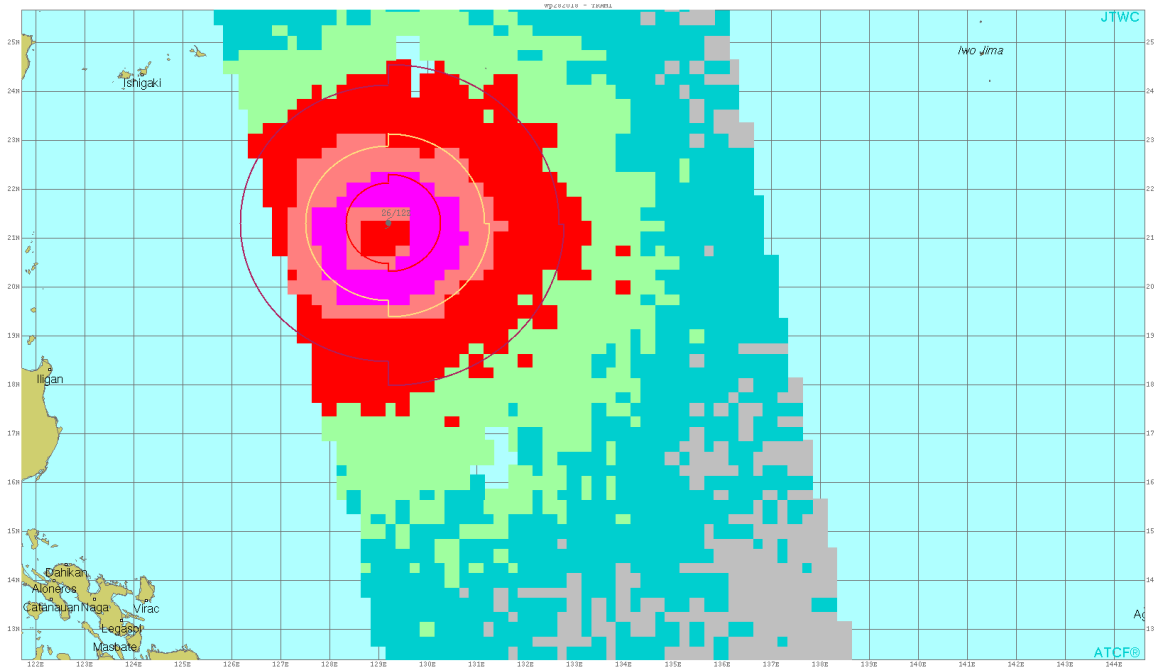
Figure 9: JTWC 34-, 50-, 64-kt wind radii (concentric radii) at 20180926 12 UTC overlaid on Soil Moisture Active Passive (SMAP) winds at 20180926 09 UTC (Meissner et al. 2017) available on operational forecast system for 28th TC of 2018 western North Pacific season.

4.1.7 Recommendations

The recommendations for guidance on wind structure and wind structure asymmetry are:

1) Develop high quality inner core wind radii observational datasets both for real-time guidance and to construct high quality post-season analyses. Not only does this include aircraft and satellite observations, but also available radars. Weather radar data has traditionally been difficult to obtain/share among forecast agencies yet provides data that could be used to augment traditionally shared data from satellite platforms.
2) Continue to bring analysis algorithms to operations, especially those which address inner core wind structure analyses and forecasts.
3) Continue to develop NWP both for analyses and forecasts of wind structure so that they can be effectively used to disseminate long-range, accurate warnings of the onset of winds, waves, swell and surge.
4) Continue to launch satellites with potential to discern wind fields.

Acronyms used in the report:

AMV – Atmospheric Motion Vector
AMSU – Advanced Microwave Sounding Unit, wind radii estimates based on AMSU
ASCAT – Advanced Scatterometer
ASCT – Objective gale wind radii fixes from ASCAT
ARCHER – Automated Rotational Center Hurricane Retrieval
AVNO/AHNI – Global Forecast System model radii analyses/interpolated forecasts
BOM - Australian Bureau of Meteorology
CHTI – COAMPS-TC model radii/interpolated forecast
CIRW – CIRA multi-platform surface wind analysis
COAMPS– Coupled Oceanographic Atmospheric Mesoscale Prediction System
COAMPS-TC – COAMPS Tropical Cyclone model
DAV – Deviation Angle Variance
DoD – U.S. Department of Defense
DRCL - Wind Radii CLIPER
DSHA – Statistical-dynamical wind radii forecasts based on GFS model data
DVRK – Dvorak estimate wind radii
EMXI – European Center model R34 interpolated forecast
ERC – Eyewall Replacement Cycle
GFDT – GFDL TC model wind analysis
GPCE – Goerss Predicted Consensus Error
INTF – Official Intensity forecast (kt), 6-h old interpolated or consensus
HWRF/HHNI – Hurricane Weather Research Forecast model radii/interpolated forecast
JMA/MSC – Japanese Meteorological Agency Meteorological Satellite Center
JTWC – Joint Typhoon Warning Center
M-PERC - Microwave Probability of Eyewall Replacement Cycle
NWP – Numerical Weather Prediction
OBTK – Objective R34, an equally-weighted average of R34 estimates
NHC – The National Hurricane Center, Miami, FL
R34 – Gale (17 m/s or 34 kt) wind radii
R50 – Storm force (25 m/s or 48 kt) wind radii
R64 – Hurricane force (33 m/s or 64 kt) wind radii
RVCN – R34 Forecast Consensus=AHNI+HHNI+EMXI+CHTI+DSHA
SFMR – Stepped Frequency Microwave Radiometer
SHIPS – Statistical Hurricane Intensity Prediction System
TC – Tropical cyclone
Vmax – Maximum wind intensity near the center of a TC

References:

Bender M. A., T. Marchok, C. Sampson, J. Knaff, and M. Morin, 2017: Impact of storm size on prediction of storm track and intensity using the 2016 operational GFDL hurricane model. *Wea. Forecasting*, https://doi.org/10.1175/WAF-D-16-0220.1.

Bentamy, A., D. Croize-Fillon, and C. Perigaud (2008), Characterization of ASCAT measurements based on buoy and QuikSCAT wind vector observations. *Ocean Sci.*, 4, 265–274.

Brennan, M. J, C. C. Hennon, and R. D. Knabb, 2009: The operational use of QuikSCAT ocean surface vector winds at the National Hurricane Center. *Wea. Forecasting,* 24, 621–645, doi: 10.1175/2008WAF2222188.1.

Cangialosi, J. P., and C. W. Landsea, 2016: An examination of model and official National Hurricane Center tropical cyclone size forecasts. Wea. Forecasting., 31, 1293-1300.

Chou, K.-H., C.-C. Wu, and S.-Z. Lin (2013), Assessment of the ASCAT wind error characteristics by global dropwindsonde observations. *J. Geophys. Res. Atmos.*, 118, 9011–9021, doi:10.1002/jgrd.50724.

Courtney. J. and A. Burton, 2018: Joint Industry Project for Objective Tropical Cyclone Reanalysis: Final Report, 87 pp. *Available from j.courtney@bom.gov.au on request.*

Davidson, N.E., Y. Xiao, Y. Ma, H.C. Weber, X. Sun, L.J. Rikus, J.D. Kepert, P.X. Steinle, G.S. Dietachmayer, C.C. Lok, J. Fraser, J. Fernon, and H. Shaik, 2014: ACCESS-TC: Vortex Specification, 4DVAR Initialization, Verification, and Structure Diagnostics. *Mon. Wea. Rev.,* **142**, 1265–1289, https://doi.org/10.1175/MWR-D-13-00062.1

DeMaria, M., J. A. Knaff, M. Brennan, D. Brown, C. Lauer, R. T. DeMaria, A. Schumacher, R. D. Knabb, D. P. Roberts, C. R. Sampson, P. Santos, D. Sharp, and K. A. Winters, 2013: Improvements to the operational tropical cyclone wind speed probability model. *Wea. Forecasting*, 28, 586-602. doi: http://dx.doi.org/10.1175/WAF-D-12-00116.1.

DeMaria, M., M. Mainelli, L.K. Shay, J.A. Knaff, and J. Kaplan, 2005: Further improvements to the Statistical Hurricane Intensity Prediction Scheme (SHIPS). *Wea. Forecasting*, 20, 531–543, https://doi.org/10.1175/WAF862.1.

Dolling, K., E. A. Ritchie, and J. S. Tyo, 2016: A Geostationary Satellite Technique to Estimate Tropical Cyclone Size. *Wea. Forecasting,* **31,** 1625-1642*.*

Knaff, J. A. and C. R. Sampson, 2015: After a decade are Atlantic tropical cyclone gale force wind radii forecasts now skillful? *Wea. Forecasting*, 30, 702–709, doi: http://dx.doi.org/10.1175/WAF-D-14-00149.1.

Knaff, J. A., C. R. Sampson, and G. Chirokova, 2017: A global statistical-dynamical tropical cyclone wind radii forecast scheme, *Wea. Forecasting, 32,* 629–644, doi: 10.1175/WAF-D-16-0168.1.

Knaff, J. A., C. J. Slocum, K. D. Musgrave, C. R. Sampson, and B. R. Strahl, 2016: Using routinely available information to estimate tropical cyclone wind structure. M*on. Wea. Rev.*, 144, 1233-1247.

Knaff, J. A., M. DeMaria, D. A. Molenar, C. R. Sampson, and M. G. Seybold, 2011: An automated, objective, multi-satellite platform tropical cyclone surface wind analysis. *J. of Applied Meteorology and Climatology.* 50, 2149-2166.

Kunii, M., 2015: Assimilation of tropical cyclone track and wind radius data with an ensemble Kalman filter. *Wea. Forecasting*, 30, 1050–1063, doi:10.1175/WAF-D-14-00088.1

Landsea, C. W., and J. L. Franklin, 2013: Atlantic hurricane database uncertainty and

presentation of a new database format. *Mon. Wea. Rev.*, 141, 3576–3592, doi:10.1175/MWR-D-12-00254.1.

Maclay, K. S., M. DeMaria, and T. H. Vonder Haar, 2008: Tropical cyclone inner core kinetic energy evolution. Mon. Wea. Rev.,136, 4882–4898.

Meissner, T., L Ricciardulli, and F.J. Wentz, 2017, Capability of the SMAP Mission to Measure Ocean Surface Winds in Storms, Bulletin of the American Meteorological Society 98(8), 1660-1677, doi: 10.1175/BAMS-D-16-0052.1.

NHC, cited 2016, Introduction to storm surge. [available on-line at http://www.nhc.noaa.gov/surge/surge_intro.pdf]

Nonaka, K., K. Shimoji, and K. Kato, 2016: Estimation of the Sea Surface Wind in the Vicinity of Typhoon Using Himawari-8 Low-Level AMVs, proceedings from the 13th International Winds Workshop, 29 June 2016, available online: http://cimss.ssec.wisc.edu/iwwg/iww13/proceedings_iww13/papers/session6/IWW13_Session6_4_Nonaka_final_update.pdf

Piñeros, M. F., E. A. Ritchie, and J. S. Tyo 2008: Objective measures of tropical cyclone structure and intensity change from remotely-sensed infrared image data. *IEEE Trans. Geosciences and remote sensing.* **46,** 3574-3580**.**

Powell, M. D., and T. A. Reinhold, 2007: Tropical cyclone destructive potential by integrated kinetic energy. *Bull. Amer. Meteor. Soc.*, 88, 513–526.

Quiring, S., A. Schumacher, and S. Guikema, 2014: Incorporating hurricane forecast uncertainty into decision support applications. *Bull. Amer. Meteor. Soc.*, 95, 47-58.

Rappaport, E. N., and Coauthors, 2009: Advances and challenges at the National Hurricane Center. Wea. Forecasting, 24, 395–419.

Ritchie, E. A., K. M. Wood, O. G. Rodriguez-Herrera, M. F. Piñeros, and J. S. Tyo, 2014: Satellite-derived tropical cyclone intensity in the North Pacific Ocean using the deviation-angle-variance technique. *Wea. Forecasting* **29,** 505-516.

Rodríguez-Herrera, O. G., K. M. Wood, K. P. Dolling, W. T. Black, E. A. Ritchie, and J. S. Tyo, 2015: Objective Automatic Storm Tracking Based on the Deviation Angle Variance Method, *IEEE Geosciences and Remote Sensing Letters,* **12,** 254-258.

Sampson, C. R., J. S. Goerss, J. A. Knaff, B. R. Strahl, E. M. Fukada, E. A. Serra, 2018: Tropical cyclone gale wind radii estimates, forecasts and error forecast for the western North Pacific, *Wea. Forecasting*, in press.

Sampson, C. R., P. A. Wittmann, and H. L. Tolman, 2010: Consistent tropical cyclone wind and wave forecasts for the U.S. Navy. *Wea. Forecasting*, 25, 1293-1306.

Sampson, C.R., A.B. Schumacher, J.A. Knaff, M. DeMaria, E.M. Fukada, C.A. Sisko, D.P. Roberts, K.A. Winters, H. M. Wilson, 2012: Objective guidance for use in setting tropical cyclone conditions of readiness. *Wea. Forecasting*, 27, 1052–1060.

Sitkowski, M., J. P. Kossin, and C. M. Rozoff, 2011: Intensity and structure changes

during hurricane eyewall replace-ment cycles. Mon. Wea. Rev.,139, 3829–3847

Tallapragada, V, L. Bernardet, M.K. Biswas, I. Ginis, Y. Kwon, Q. Liu, T. Marchok, D. Sheinin, B. Thomas, M. Tong, S. Trahan, W. Wang, R. Yablonsky, and Z. Zhang, 2015: Hurricane Weather Research and Forecasting (HWRF) Model: 2015 scientific documentation, August 2015 – HWRF v3.7a. NCAR Developmental Testbed Center: Boulder, CO. 123pp [available on-line at http://www.dtcenter.org/HurrWRF/users/docs/scientific_documents/HWRF_v3.7a_SD.pdf].

Torn, R. and C. Snyder, 2012: Uncertainty of tropical cyclone best-track information. *Wea. Forecasting*, 27, 715–729, doi: 10.1175/WAF-D-11-00085.1.

Wimmers, A., C. Velden 2015: Advancements in Objective Multisatellite Tropical Cyclone Center Fixing. *J. Appl. Meteor and Clim*, **55**, 197-212.

___ and C. Velden, 2010: Objectively Determining the Rotational Center of Tropical Cyclones in Passive Microwave Satellite Imagery. *J. Appl. Meteor and Clim*. **49**, 2013-2034.

Wood, K. M, O. G. Rodriguez-Herrera, E. A. Ritchie, M. F. Piñeros, I. A. Hernández, and J. S. Tyo, 2015: Tropical cyclogenesis detection in the North Pacific using the deviation angle variance technique. *Wea. Forecasting,* **30,** 1663-1672. doi: http://dx.doi.org/10.1175/WAF-D-14-00113.1